

1 High-Energy Physics Tools for Effective Field Theories¹

1.1 Introduction

The discovery by the ATLAS and CMS collaborations of a Higgs boson with a mass of about 125 GeV [1, 2] has marked an important step forward in the study and the understanding of the electroweak symmetry breaking mechanism. Although the currently measured properties of this newly discovered boson seem to be compatible with the Standard Model expectation, the recent start of the second LHC experimental run has risen new hopes to detect phenomena beyond the Standard Model. In this context, present and future LHC data could be interpreted in an effective field theory framework where departures from the Standard Model are organized as a series expansion in the new physics energy scale Λ that is assumed to be large.

The leading effects implied by such an effective field theory description usually consist of dimension-six operators that are supplemented to the Standard Model Lagrangian, each of these being associated with a new interaction strength. The number of independent coefficients is usually large, but important classes of observables turn to only depend on a much smaller subset of parameters. The effective field theory approach is therefore testable and the results could be reinterpreted to constrain explicit new physics models. Consequently, the development of high-energy physics tools able to perform computations in the effective field theory context has been a very active field during the last decades. Recent progress addresses precision calculations for the production cross section of a single Higgs boson (see Section 1.2) and a pair of Higgs bosons (see Section 1.3), and for Higgs decays (see Section 1.4). In addition, machineries have been built so that we are now able to characterize Higgs decays by means of pseudo-observables (see Section 1.5), as well as all Higgs properties by means of Monte Carlo event generation within the MADGRAPH5_aMC@NLO platform (see Section 1.6). Monte Carlo simulations can also be performed with the VBFNLO program, that includes both next-to-leading order QCD and higher-dimensional operator effects to vector boson fusion processes (see Section 1.7), and with the WHIZARD package at the leading-order accuracy (see Section 1.8). As all codes are using different conventions, we review the notation in each case.

An important aspect of the effective field theory approach is the freedom in the choice of the operator basis, so that a given effect could be modeled by several different combinations of operators at a fixed order in the effective energy scale expansion. This is related to the possibility of redefining the Standard Model fields in such a way that the Standard Model Lagrangian is unaltered, while certain combinations of dimension-six operators proportional to the Standard Model equations of motion can be eliminated up to subleading higher-dimensional effects. Different complete operator bases have been proposed in the past, and although each of them yields the same predictions, they present specific and different advantages. Existing calculations or tools are however often bound to a given basis choice, and it is desirable to be able to reuse results derived in the context of one basis in another basis. The ROSETTA platform (see Section 1.9) has been very recently released to close this gap.

1.2 HIGLU: Higgs Boson Production via Gluon Fusion

The program HIGLU [3, 4] calculates the Higgs boson production cross section via gluon-fusion up to the next-to-next-to-leading order (NNLO) accuracy in QCD [5–15] and includes next-to-leading order (NLO) electroweak corrections [16–24] within the Standard Model, and up to the NNLO in QCD [5–15, 25–34] for the minimal supersymmetric extension of the Standard Model. While the supersymmetric electroweak corrections are unknown, the known genuine supersymmetric QCD corrections [35–45] are not included in the program. Starting from the Standard Model Higgs results, the contributions of dimension-six operators beyond the Standard Model are included up to the NNLO in QCD. The latter extension is based on the effective Lagrangian (in the heavy top limit for the Standard Model part) [46–49],

$$\mathcal{L}_{\text{eff}} = \frac{\alpha_s}{\pi} \left[\frac{c_t}{12} (1 + \delta) + c_g \right] G_a^{\mu\nu} G_{\mu\nu}^a \frac{H}{v}, \quad (1)$$

where H denotes the Standard Model physical Higgs boson and v the vacuum expectation value of the neutral component of the Higgs field Φ . Moreover, the gluon field strength tensor is denoted by $G_a^{\mu\nu}$ and the strong coupling constant by α_s . The contributions of dimension-six operators are absorbed in the rescaling factor c_t for the top Yukawa coupling and the point-like coupling c_g . In other words, deviations of c_t and c_g from their Standard Model values $c_t = 1$ and $c_g = 0$ are understood to originate from dimension-six operators. The contribution of the chromomagnetic dipole operator [50, 51] is not included. The Lagrangian above includes QCD corrections via the δ parameter,

$$\delta = \delta_1 \frac{\alpha_s}{\pi} + \delta_2 \left(\frac{\alpha_s}{\pi} \right)^2 + \delta_3 \left(\frac{\alpha_s}{\pi} \right)^3, \quad (2)$$

¹ B. Fuks (ed.); F. Campanario, B. Chokoufe, R. Contino, F. Demartin, A. Falkowski, M. Ghezzi, A. Greljo, R. Gröber, C. Grojean, G. Isidori, W. Kilian, D. Marzocca, K. Mawatari, K. Mimasu, M. Mühlleitner, T. Ohl, G. Perez, M. Rauch, J. Reuter, F. Riva, R. Roth, V. Sanz, M. Sekulla, S. So Young, C. Speckner, M. Spira, J. Streicher, C. Weiss, M. Zaro, D. Zeppenfeld

47 whose three components read

$$\begin{aligned}
\delta_1 &= \frac{11}{4}, & \delta_2 &= \frac{2777}{288} + \frac{19}{16}L_t + N_F \left(\frac{L_t}{3} - \frac{67}{96} \right), \\
\delta_3 &= \frac{897943}{9216}\zeta_3 - \frac{2761331}{41472} + \frac{209}{64}L_t^2 + \frac{2417}{288}L_t + N_F \left(\frac{58723}{20736} - \frac{110779}{13824}\zeta_3 + \frac{23}{32}L_t^2 + \frac{91}{54}L_t \right) \\
&\quad + N_F^2 \left(-\frac{L_t^2}{18} + \frac{77}{1728}L_t - \frac{6865}{31104} \right),
\end{aligned} \tag{3}$$

48 where $L_t = \log(\mu_R^2/m_t^2)$ with μ_R denoting the renormalization scale, N_F the number of active quark flavors and m_t the
49 top quark pole mass.

50 The leading order (LO) cross section extended by the new physics contributions induced by the above effective La-
51 grangian is given by

$$\sigma_{LO}(pp \rightarrow H) = \sigma_0 \tau_H \frac{d\mathcal{L}^{gg}}{d\tau_H}, \tag{4}$$

52 where \mathcal{L}^{gg} stands for the gluon-gluon partonic luminosity and where $\tau_H = m_h^2/S$, m_h being the Higgs-boson mass and
53 S the hadronic center-of-mass energy. The σ_0 prefactor can be computed either in the non-linear case (σ_0^{NL}) or in the
54 SILH (strongly interacting light Higgs) framework (σ_0^{SILH}),

$$\sigma_0^{\text{NL}} = \frac{G_F \alpha_s^2}{288\sqrt{2}\pi} \left| \sum_Q c_Q A_{1/2}(\tau_Q) + 12c_g \right|^2 \quad \text{and} \quad \sigma_0^{\text{SILH}} = \sigma_0^{\text{NL}} - \frac{G_F \alpha_s^2}{288\sqrt{2}\pi} \left| \sum_Q (c_Q - 1) A_Q(\tau_Q) + 12c_g \right|^2, \tag{5}$$

55 where $\tau_Q = 4m_Q^2/m_h^2$ with m_Q being a generic quark mass, and where $G_F = (\sqrt{2}v^2)^{-1}$ stands for the Fermi constant.
56 The LO form factors depend on the $A_{1/2}$ function that is given by

$$A_{1/2}(\tau) = \frac{3}{2}\tau \left[1 + (1-\tau)f(\tau) \right] \quad \text{with} \quad f(\tau) = \begin{cases} \arcsin^2 \frac{1}{\sqrt{\tau}} & \text{for } \tau \geq 1 \\ -\frac{1}{4} \left[\ln \frac{1+\sqrt{1-\tau}}{1-\sqrt{1-\tau}} - i\pi \right]^2 & \text{for } \tau < 1. \end{cases} \tag{6}$$

57 Rescaling factors c_Q have been introduced in Eq. (5) for all contributing quarks, *i.e.*, the top (c_t), bottom (c_b) and charm
58 (c_c) quarks.

59 The Wilson coefficient c_g does not receive QCD corrections within the effective Lagrangian, but develops a scale
60 dependence according to the renormalization group equation

$$\mu^2 \frac{\partial c_g(\mu^2)}{\partial \mu^2} = - \left\{ \beta_1 \left(\frac{\alpha_s(\mu^2)}{\pi} \right)^2 + 2\beta_2 \left(\frac{\alpha_s(\mu^2)}{\pi} \right)^3 \right\} c_g(\mu^2), \tag{7}$$

61 with

$$\beta_0 = \frac{33 - 2N_F}{12}, \quad \beta_1 = \frac{153 - 19N_F}{24} \quad \text{and} \quad \beta_2 = \frac{1}{128} \left(2857 - \frac{5033}{9}N_F + \frac{325}{27}N_F^2 \right). \tag{8}$$

62 This renormalization group equation can be derived either from the scale-invariant trace anomaly term
63 $\beta(\alpha_s)/\alpha_s G_a^{\mu\nu} G_{\mu\nu}^a$ [52–57], or from the scale dependence of the factor $(1 + \delta)$ of the effective Lagrangian of Eq. (1),
64 since both coefficients, $c_t(1 + \delta)$ and c_g , have to develop the same scale dependence. The solution of the RGE for c_g up
65 to the next-to-next-to-leading logarithmic (NNLL) level can be cast into the form

$$c_g(\mu^2) = c_g(\mu_0^2) \frac{\beta_0 + \beta_1 \frac{\alpha_s(\mu^2)}{\pi} + \beta_2 \left(\frac{\alpha_s(\mu^2)}{\pi} \right)^2}{\beta_0 + \beta_1 \frac{\alpha_s(\mu_0^2)}{\pi} + \beta_2 \left(\frac{\alpha_s(\mu_0^2)}{\pi} \right)^2}. \tag{9}$$

66 In order to compute the modified cross section up to NNLO, the mismatch of the individual terms of the effective La-
67 grangian of Eq. (1) with respect to the δ terms have been taken into account, the NNLL scale dependence of the Wilson
68 coefficient c_g being properly included. In addition, the finite NLO quark mass term effects have been added at fixed NLO
69 to the Standard Model contributions. This yields a consistent determination of the gluon-fusion cross section up to NNLO
70 including the dimension-six operators that imply a rescaling of the top, bottom and charm Yukawa couplings and the
71 point-like Hgg coupling parameterized by $c_g(\mu_R^2)$.

72 The present version 4.31 of HIGLU is linked to HDECAY (version 6.50) [58, 59] and allows one to choose the usual
73 Standard Model Higgs input values in the separate input files `higlu.in` and `hdecay.in`. In addition, the rescaling

74 factors $c_{t,b,c}$ and the point-like Wilson coefficient $c_g(\mu_0^2)$ can be set, together with the corresponding input scale μ_0 , in
75 the `higlu.in` file. In this way, HIGLU provides a consistent calculation of the gluon-fusion cross section up to NNLO
76 QCD including dimension-six operator effects. More detailed information about the input files `higlu.in` and `hdecay.in`
77 can be found as comment lines at the beginning of the main FORTRAN files `higlu.f` and `hdecay.f` shipped with the
78 program. Finally, we note that the pole masses of the bottom and charm quarks are computed from the $\overline{\text{MS}}$ input values
79 $\overline{m}_b(\overline{m}_b)$ and $\overline{m}_c(3 \text{ GeV})$ with N³LO accuracy internally.

80 1.3 HPAIR: Higgs Boson Pair Production via Gluon Fusion

81 The program HPAIR, available at

82 <http://tiger.web.psi.ch/hpair/>,

83 calculates the Higgs boson pair production cross section via gluon fusion up to the NLO in QCD [60] in the limit of
84 heavy top quarks within the Standard Model and the quark-loop induced contributions in the minimal supersymmetric
85 extension of the Standard Model. While genuine supersymmetric QCD and electroweak corrections are unknown, known
86 subleading NLO top mass effects [61–64] and NNLO QCD corrections [65–67] are not included in the program. Starting
87 from the Standard Model Higgs result in the heavy top mass limit, the contributions of dimension-six operators beyond the
88 Standard Model are included up to the NLO in QCD [68]. The latter extension is based on an effective phenomenological
89 Lagrangian given by

$$\mathcal{L}_{\text{eff}} = -m_t \bar{t} t \left[c_t \frac{H}{v} + c_{tt} \frac{H^2}{2v^2} \right] - \frac{1}{6} c_3 \left[\frac{3m_h^2}{v} \right] H^3 + \frac{\alpha_s}{\pi} G_a^{\mu\nu} G_{\mu\nu}^a \left[c_g \frac{H}{v} + c_{gg} \frac{H^2}{2v^2} \right], \quad (10)$$

90 As in Section 1.2, the contributions of the dimension-six operators are absorbed in the rescaling factors c_t for the top
91 Yukawa coupling and c_3 for the trilinear Higgs coupling, *i.e.*, deviations of c_t and c_3 from the Standard Model expectation
92 of $c_t = c_3 = 1$ originate from dimension-six operators. The remaining couplings c_{tt} , c_g and c_{gg} are novel contributions
93 purely arising from dimension-six operators and not present in the Standard Model Lagrangian. Integrating out the heavy
94 top quark loops one arrives at the effective Lagrangian

$$\mathcal{L}_{\text{eff}} = \frac{\alpha_s}{\pi} G_a^{\mu\nu} G_{\mu\nu}^a \left\{ \frac{H}{v} \left[\frac{c_t}{12} \left(1 + \frac{11}{4} \frac{\alpha_s}{\pi} \right) + c_g \right] + \frac{H^2}{v^2} \left[\frac{c_{tt} - c_t^2}{24} \left(1 + \frac{11}{4} \frac{\alpha_s}{\pi} \right) + \frac{c_{gg}}{2} \right] \right\}, \quad (11)$$

95 describing the Higgs couplings to gluons when only the leading QCD corrections for the single Higgs interactions are
96 kept (compared to Eq. (1)).

97 The partonic LO cross section extended by beyond the Standard Model contributions induced by the above Lagrangian
98 is given by

$$\hat{\sigma}_{LO}(gg \rightarrow HH) = \int_{\hat{t}_-}^{\hat{t}_+} d\hat{t} \frac{G_F^2 \alpha_s^2(\mu_R)}{256(2\pi)^3} \left[|C_\Delta F_1 + F_2|^2 + |c_t^2 G_\square|^2 \right], \quad (12)$$

99 where the Mandelstam variables are defined by

$$\hat{s} = Q^2, \quad \hat{t} = m_h^2 - \frac{Q^2(1 - \beta \cos \theta)}{2} \quad \text{and} \quad \hat{u} = m_h^2 - \frac{Q^2(1 + \beta \cos \theta)}{2}, \quad (13)$$

100 with $\beta = \sqrt{1 - 4m_h^2/Q^2}$ and with Q denoting the invariant mass of the Higgs boson pair. Moreover, the integration
101 bounds at $\cos \theta = \pm 1$ read

$$\hat{t}_\pm = m_h^2 - \frac{Q^2(1 \mp \beta)}{2}. \quad (14)$$

102 The form factors F_1 and F_2 can be cast into the form

$$F_1 = c_t F_\Delta + \frac{2}{3} c_\Delta \quad \text{and} \quad F_2 = c_t^2 F_\square + c_{tt} F_\Delta - \frac{2}{3} c_\square, \quad (15)$$

103 with the explicit expressions of F_Δ , F_\square and G_\square being available in Ref. [69, 70]. In the limit of heavy top quarks they
104 simplify to

$$F_1^{\text{lim}} = \frac{2}{3} (c_t + c_\Delta), \quad F_2^{\text{lim}} = \frac{2}{3} (-c_t^2 + c_{tt} - c_\square), \quad (16)$$

105 after introducing the abbreviations c_Δ and c_\square . The latter read, together with the C_Δ variable of Eq. (12),

$$C_\Delta \equiv \lambda_{hhh} \frac{m_Z^2}{Q^2 - m_h^2 + im_h \Gamma_h}, \quad c_\Delta \equiv 12c_g \quad \text{and} \quad c_\square \equiv -12c_{gg}, \quad (17)$$

106 with m_Z denoting the Z -boson mass, Γ_h the Higgs boson width, and the trilinear Higgs coupling being normalized as

$$\lambda_{hhh} = \frac{3m_h^2 c_3}{m_Z^2}. \quad (18)$$

107 The partonic cross section has then to be convoluted with the gluon density in the proton in order to obtain the hadronic
108 cross section.

109 The present version 2.00 of HPAIR needs the usual Standard Model Higgs input values that are provided in a separate
110 input file `hpair.in`. In addition, this file also allows one for choosing the anomalous dimension-six factors c_t, c_{tt}, c_g, c_{gg}
111 and c_3 . Alternatively the dimension-six coefficients $\bar{c}_H, \bar{c}_u, \bar{c}_6$ and \bar{c}_g can be provided within the usual SILH basis [71],
112 starting from the effective SILH Lagrangian

$$\Delta\mathcal{L}_6^{\text{SILH}} \supset \frac{\bar{c}_H}{2v^2} \partial_\mu(\Phi^\dagger\Phi)\partial^\mu(\Phi^\dagger\Phi) + \frac{\bar{c}_u}{v^2} y_t \left(\Phi^\dagger\Phi\bar{q}_L\Phi^c t_R + \text{h.c.} \right) - \frac{\bar{c}_6}{6v^2} \frac{3m_h^2}{v^2} \left(\Phi^\dagger\Phi \right)^3 + \bar{c}_g \frac{g_s^2}{m_W^2} \Phi^\dagger\Phi G_{\mu\nu}^a G_a^{\mu\nu}, \quad (19)$$

113 where $y_t = \sqrt{2}m_t/v$ denotes the top quark Yukawa coupling, g_s the strong coupling constant and m_W the W -boson
114 mass. The connection to the Lagrangian of Eq. (10) is given by

$$c_t = 1 - \frac{\bar{c}_H}{2} - \bar{c}_u, \quad c_{tt} = -\frac{1}{2}(\bar{c}_H + 3\bar{c}_u), \quad c_3 = 1 - \frac{3}{2}\bar{c}_H + \bar{c}_6, \quad c_g = c_{gg} = \bar{c}_g \frac{4\pi}{\alpha_2}, \quad (20)$$

115 with $\alpha_2 = \sqrt{2}G_F m_W^2/\pi$. Contrary to the strongly interacting non-linear case, in the SILH case products of dimension-six
116 coefficients are not taken into account in accordance with a consistent expansion of the physical observable up to linear
117 dimension-six terms. In the SILH case, this also requires the expansion of the LO cross section of Eq. (12) up to linear
118 dimension-six terms. The NLO terms are treated accordingly in the HPAIR program that allows for both options, *i.e.*, the
119 non-linear and SILH cases. In this way, HPAIR provides a consistent calculation of the gluon-fusion cross section up to
120 NLO QCD including the effects of dimension-six operators. More detailed information about the input file `hpair.in` can
121 be found as comment lines at the beginning of the main FORTRAN file `hpair.f` shipped with the program.

122 1.4 eHDECAY, Higgs Decays in the Effective Lagrangian Approach

123 In Ref. [72], we have presented the program eHDECAY, a FORTRAN code based on a modification of the program HDE-
124 CAY [58, 59], and discussed the relation between the non-linear and the linear effective Lagrangian approaches. The
125 program can be downloaded from

126 <http://www.itp.kit.edu/~maggie/eHDECAY/>.

127 In eHDECAY, the full list of leading bosonic operators of the Higgs effective Lagrangian has been implemented, both for
128 a linear and a non-linear realization of the electroweak symmetry and for two benchmark composite Higgs models called
129 MCHM4 [73] and MCHM5 [74]. All the relevant QCD corrections have been included and we detail in the following the
130 importance of higher-order QCD corrections and of mass effects on the corrections. We also show how to consistently
131 include electroweak corrections whenever it is possible, focusing on the example of the Higgs boson decay into two glu-
132 ons. As the leading part of the QCD corrections in general factorizes with respect to the expansion in the number of fields
133 and derivatives of the effective Lagrangian, they can be included by taking over the results from the Standard Model. The
134 electroweak corrections, on the contrary, require dedicated computations that are only partly available at present. They
135 are consequently only implemented up to higher orders in a v^2/f^2 expansion in the framework of the linear Lagrangian,
136 where $f = \Lambda/g_*$ with g_* being a typical new physics coupling strength. They are valid, for instance, in the SILH frame-
137 work [71] in which the deviations from the Standard Model are small. On different lines, higher-order QCD corrections
138 and mass effects are included also in the non-linear implementation.

139 Denoting by c_ψ the modifications of the Higgs couplings to fermions with respect to the Standard Model and by c'_{gg}
140 the effective Higgs coupling to gluons, the related non-linear effective Lagrangian reads

$$\Delta\mathcal{L}_{\text{NL}} = - \sum_{\psi=u,d,\ell} c_\psi m_\psi \bar{\psi}\psi \frac{h}{v} + \frac{c'_{gg}}{2} G_{\mu\nu}^a G_a^{\mu\nu} \frac{h}{v}. \quad (21)$$

141 The decay rate into gluons implemented in eHDECAY in the framework of the non-linear Lagrangian is then given by

$$\Gamma_{gg}^{\text{NL}} = \frac{G_F \alpha_s^2 m_h^3}{4\sqrt{2}\pi^3} \left[\left| \sum_{q=t,b,c} \frac{c_q}{3} A_{1/2}(\tau_q) \right|^2 c_{\text{eff}}^2 \kappa_{\text{soft}} + 2 \operatorname{Re} \left\{ \sum_{q=t,b,c} \frac{c_q}{3} A_{1/2}^*(\tau_q) \frac{2\pi c_{gg}}{\alpha_s} \right\} c_{\text{eff}} \kappa_{\text{soft}} + \left| \frac{2\pi c_{gg}}{\alpha_s} \right|^2 \kappa_{\text{soft}} \right. \\ \left. + \frac{1}{9} \sum_{q,q'=t,b} c_q A_{1/2}^*(\tau_q) c_{q'} A_{1/2}(\tau_{q'}) \kappa^{\text{NLO}}(\tau_q, \tau_{q'}) \right]. \quad (22)$$

142 On the other hand, the part of the linear Lagrangian that contributes to the Higgs boson decay into two gluons reads, in
143 the SILH basis,

$$\Delta\mathcal{L}_6^{\text{SILH}} \supset \frac{\bar{c}_H}{2v^2} \partial^\mu(\Phi^\dagger\Phi)\partial_\mu(\Phi^\dagger\Phi) + \frac{\bar{c}_g g_s^2}{m_W^2} \Phi^\dagger\Phi G_{\mu\nu}^a G_a^{\mu\nu} + \left(\frac{\bar{c}_u y_u}{v^2} \Phi^\dagger\Phi\bar{q}_L\Phi^c u_R + \frac{\bar{c}_d y_d}{v^2} \Phi^\dagger\Phi\bar{q}_L\Phi^c d_R + \text{h.c.} \right), \quad (23)$$

144 where \bar{c}_H , \bar{c}_g , \bar{c}_u and \bar{c}_d are the Wilson coefficients of the corresponding dimension-six effective operators and $y_{u,d}$ the
 145 Yukawa couplings of the up- and down-type quarks, respectively. In this case, the Higgs boson decay rate into gluons
 146 implemented in eHDECAY is given by

$$\begin{aligned} \Gamma_{gg}^{\text{SILH}} = & \frac{G_F \alpha_s^2 m_h^3}{4\sqrt{2}\pi^3} \left[\frac{1}{9} \sum_{q,q'=t,b,c} (1 - \bar{c}_H - \bar{c}_q - \bar{c}_{q'}) A_{1/2}^*(\tau_{q'}) A_{1/2}(\tau_q) c_{\text{eff}}^2 \kappa_{\text{soft}} \right. \\ & + 2 \operatorname{Re} \left\{ \sum_{q=t,b,c} \frac{1}{3} A_{1/2}^*(\tau_q) \frac{16\pi\bar{c}_g}{\alpha_2} \right\} c_{\text{eff}} \kappa_{\text{soft}} + \left| \sum_{q=t,b,c} \frac{1}{3} A_{1/2}(\tau_q) \right|^2 c_{\text{eff}}^2 \kappa_{\text{ew}} \kappa_{\text{soft}} \\ & \left. + \frac{1}{9} \sum_{q,q'=t,b} (1 - \bar{c}_H - \bar{c}_q - \bar{c}_{q'}) A_{1/2}^*(\tau_q) A_{1/2}(\tau_{q'}) \kappa^{\text{NLO}}(\tau_q, \tau_{q'}) \right]. \end{aligned} \quad (24)$$

147 In both Eq. (22) and Eq. (24), $\tau_q = 4m_q^2/m_h^2$ and the loop function $A_{1/2}(\tau)$ is defined as in Eq. (6). We use the pole
 148 masses for the top, bottom and charm quark masses and α_s is computed up to N³LO at a scale fixed to m_h and for $N_F = 5$
 149 active flavors. The QCD corrections have been taken into account up to N³LO in QCD in the limit of heavy loop-particle
 150 masses so that the effect from low-energy gluon radiation, given by the coefficient κ_{soft} , factorizes in this limit. The
 151 corrections from high-energy gluon and quark exchange (with virtuality $q^2 \gg m_t^2$) are encoded in the coefficient c_{eff} .
 152 Namely, for $m_h \ll 2m_t$, the top quark can be integrated out, leading to the effective five-flavor Lagrangian

$$\mathcal{L}_{\text{eff}} = -2^{1/4} G_F^{1/2} C_1 G_{\mu\nu}^a G_a^{\mu\nu} h, \quad (25)$$

153 where the dependence on the top quark mass m_t is included in the coefficient function C_1 . We then have

$$\kappa_{\text{soft}} = \frac{\pi}{2m_h^4} \operatorname{Im} \{ \Pi^{GG}(q^2 = m_h^2) \} \quad \text{and} \quad c_{\text{eff}} = -\frac{12\pi C_1}{\alpha_s(m_h)}, \quad (26)$$

154 with the vacuum polarization $\Pi^{GG}(q^2)$ being induced by the gluon operator. The N³LO expressions for C_1 and for
 155 $\operatorname{Im}\{\Pi^{GG}\}$ have been given in Refs. [47, 48, 75, 76] and Ref. [77], respectively. In particular, the NLO expressions for
 156 κ_{soft} and c_{eff} read [5, 78, 79]

$$\kappa_{\text{soft}}^{\text{NLO}} = 1 + \frac{\alpha_s}{\pi} \left(\frac{73}{4} - \frac{7}{6} N_F \right) \quad \text{and} \quad c_{\text{eff}}^{\text{NLO}} = 1 + \frac{\alpha_s}{\pi} \frac{11}{4}, \quad (27)$$

157 in agreement with the low-energy theorem [80–82]. The additional mass effects at NLO [8] in the top and bottom quark
 158 loops are taken into account by the function $\kappa^{\text{NLO}}(\tau_q, \tau_{q'})$ in the last lines of Eqs. (22) and (24). This function quantifies
 159 the difference between the NLO QCD corrections for the top (bottom) contribution taking into account finite mass effects
 160 in the loop, and the result for the top (bottom) contribution in the limit of a large loop-particle mass.

161 Higher order corrections are large, with in particular the N³LO QCD corrections increasing the total width by almost
 162 up to 90%. The mass effects at NLO QCD are relevant for the bottom loop where they amount to 8%, while they are
 163 negligible for the top loop. To be consistent with the non-linear approach, no electroweak corrections have been included
 164 in the non-linear parameterization, as a perturbative expansion in powers of v^2/f^2 is not possible in the general case.
 165 In contrast, in the linear parameterization, we have included both QCD and electroweak corrections. The treatment of
 166 the QCD corrections is in accordance with the non-linear case, while the electroweak corrections [16–23] are taken into
 167 account by the factor κ_{ew} of Eq. (24). In the Standard Model, they can be factorized in the particular case of the Higgs
 168 boson decaying into two gluons. However, this factorization is not valid in the general case. In particular, when the
 169 contributions from the effective Lagrangian are taken into account, modified Higgs couplings absent at the leading order
 170 can appear and spoil the factorization. Hence, a consistent inclusion of the electroweak corrections is only possible in the
 171 linear-Lagrangian case and up to higher orders in v^2/f^2 . More precisely, the Standard Model electroweak corrections can
 172 be added to get a result that includes the leading $\mathcal{O}(v^2/f^2)$ and the next-to-leading $\mathcal{O}(\alpha/4\pi)$ corrections as well as the
 173 mixed $\mathcal{O}[(\alpha_s/4\pi)^5(\alpha/4\pi)]$ contributions, but that neglects terms of $\mathcal{O}[(\alpha/4\pi)(v^2/f^2)]$, $\mathcal{O}[(v^2/f^2)^2]$ and $\mathcal{O}[(\alpha/4\pi)^2]$,
 174 where α is generically meant as the electroweak expansion parameter.

175 For the future we are planning to add to eHDECAY contributions from the fermionic effective operators and those
 176 from the effective Lagrangian to the set of input observables m_W , m_Z and G_F . Moreover, in accordance with the
 177 Higgs Cross Section Working Group Internal Note of Ref. [83], a switch from the pole-mass scheme to the $\overline{\text{MS}}$ scheme
 178 for the fermionic masses is under consideration, as well as the implementation of an interface for the so-called ‘Higgs
 179 basis’ (Ref. to the WG2 chapter) parameterization of the effective Lagrangian (see also Section 1.9).

180 1.5 Implementation of Higgs Pseudo-Observables in the Universal FEYNRULES Output

181 With the upcoming LHC Run-II, Higgs physics is entering a precision era. This would allow us to look for new physics
 182 effects not only in the overall signal strengths, but also in kinematical distributions. In this perspective, the so called ‘ κ -
 183 framework’ [84] is insufficient and needs to be extended. The natural extension is the so-called Higgs pseudo-observables

Process	$h \rightarrow bb$	$h \rightarrow \tau\tau$	$h \rightarrow cc$	$h \rightarrow \mu\mu$
Pseudo-observables	$\kappa_b, \lambda_b^{\text{CP}}$	$\kappa_\tau, \lambda_\tau^{\text{CP}}$	$\kappa_c, \lambda_c^{\text{CP}}$	$\kappa_\mu, \lambda_\mu^{\text{CP}}$

Table 1: Pseudo-observables relevant for Higgs decays into two fermions.

Process	Pseudo-observables
$h \rightarrow \gamma\gamma$	$\kappa_{\gamma\gamma}, \lambda_{\gamma\gamma}^{\text{CP}}$
$h \rightarrow Z\gamma$	$\kappa_{Z\gamma}, \lambda_{Z\gamma}^{\text{CP}}$
$h \rightarrow \gamma 2\nu$	$\kappa_{Z\gamma}, \lambda_{Z\gamma}^{\text{CP}}$
$h \rightarrow \gamma 2\ell$	$\kappa_{\gamma\gamma}, \lambda_{\gamma\gamma}^{\text{CP}}, \kappa_{Z\gamma}, \lambda_{Z\gamma}^{\text{CP}}$
$h \rightarrow Z 2\ell$	$\kappa_{ZZ}, \epsilon_{ZZ}, \epsilon_{ZZ}^{\text{CP}}, \kappa_{Z\gamma}, \lambda_{Z\gamma}^{\text{CP}}, \epsilon_{Z\ell_L}, \epsilon_{Z\ell_R}$
$h \rightarrow 2\ell 2\ell'$	$\kappa_{ZZ}, \epsilon_{ZZ}, \epsilon_{ZZ}^{\text{CP}}, \kappa_{Z\gamma}, \lambda_{Z\gamma}^{\text{CP}}, \kappa_{\gamma\gamma}, \lambda_{\gamma\gamma}^{\text{CP}}, \epsilon_{Z\ell_L}, \epsilon_{Z\ell_R}, \epsilon_{Z\ell'_L}, \epsilon_{Z\ell'_R}$
$h \rightarrow 4\ell$	$\kappa_{ZZ}, \epsilon_{ZZ}, \epsilon_{ZZ}^{\text{CP}}, \kappa_{Z\gamma}, \lambda_{Z\gamma}^{\text{CP}}, \kappa_{\gamma\gamma}, \lambda_{\gamma\gamma}^{\text{CP}}, \epsilon_{Z\ell_L}, \epsilon_{Z\ell_R}$
$h \rightarrow \bar{\ell}\ell 2\nu$	$\left\{ \begin{array}{l} \kappa_{ZZ}, \epsilon_{ZZ}, \epsilon_{ZZ}^{\text{CP}}, \kappa_{Z\gamma}, \lambda_{Z\gamma}^{\text{CP}}, \epsilon_{Z\ell_L}, \epsilon_{Z\ell_R}, \epsilon_{Z\nu} \\ \kappa_{WW}, \epsilon_{WW}, \epsilon_{WW}^{\text{CP}}, \epsilon_{W\ell}, \phi_{W\ell} \end{array} \right.$
$h \rightarrow \bar{\ell}'\ell' 2\nu$	$\kappa_{WW}, \epsilon_{WW}, \epsilon_{WW}^{\text{CP}}, \epsilon_{W\ell}, \phi_{W\ell}, \epsilon_{W\ell'}, \phi_{W\ell'}$

Table 2: Pseudo-observables relevant for Higgs decays into a gauge-boson pair, and into a three-body or four-body system. We denote by ℓ an electron, a muon or a tau and ν indicates any of the three neutrino species.

184 framework introduced in Refs. [85, 86]. A detailed discussion about this formalism is presented elsewhere in this Yellow
185 Report 4. Here we limit ourselves to summarize its main features in order to illustrate its implementation via the Universal
186 FEYNRULES Output model HIGGSPO that is available at
187 <http://www.physik.uzh.ch/data/HiggsPO>.

188 The pseudo-observables are a finite set of parameters that are experimentally accessible, well-defined from the point of
189 view of a quantum field theory, and that characterize possible deviations from the Standard Model in processes involving
190 the Higgs boson in great generality. More precisely, the Higgs pseudo-observables are defined from a general decom-
191 position (based on analyticity, unitarity, and crossing symmetry) of on-shell amplitudes involving the Higgs boson and a
192 momentum expansion following the assumption of no new light particles in the kinematical regime where the decompo-
193 sition is assumed to be valid. A further key assumption of the pseudo-observables formalism is that the Higgs boson is a
194 spin zero resonance with a narrow width, such that new physics effects in production and decay factorize.

195 Due to their simple kinematics, two-body Higgs decays (into a $\gamma\gamma$ and an $\bar{f}f$ pair) can be parameterized by only two
196 pseudo-observables each, one describing the CP -conserving amplitude and another for the CP -violating one. Unless the
197 polarization of the final states can be measured, only a combination of the two is experimentally accessible. Three-body
198 and four-body Higgs decays (such as into $2\ell\gamma$, 4ℓ and $2\ell 2\nu$ systems) have a more complicated kinematics. In this case the
199 pseudo-observables are defined from the expansion of the on-shell amplitudes around the known physical poles due to the
200 propagation of intermediate Standard Model electroweak gauge bosons. General amplitude decomposition and pseudo-
201 observables definitions can be found in Ref. [85] for the Higgs decays and in Ref. [86] for Higgs boson production in the
202 vector-boson fusion mode and in association with a gauge boson.

203 The pseudo-observables are defined directly at the amplitude level. As such, on the one hand they can be computed
204 from a specific Lagrangian (to a specific order in perturbation theory), and on the other hand the pseudo-observables are
205 directly connected to S -matrix elements, providing a direct link to physical observables [85]. They are thus particularly
206 well suited for the analysis of experimental data with the matrix-element method [87]. In order to use the pseudo-
207 observable decomposition for precision studies, it is important to account for the long-distance contributions due to soft
208 and collinear photon emission (*i.e.*, the leading QED radiative corrections). These represent a universal correction factor
209 that can be implemented, by means of appropriate convolution functions or, equivalently, by showering algorithms in
210 Monte Carlo simulations, irrespective of the specific short-distance structure of the amplitude. It has been shown that
211 inclusion of such correction in $h \rightarrow 2e2\mu$ decays recovers the complete NLO Standard Model predictions within an
212 accuracy of about 1% [88].

213 In order to use the pseudo-observable framework in experimental analyses, it is convenient to have a tool capable of
214 generating signal events for specific values of the pseudo-observables. Such a tool has been developed in the context of
215 the Higgs decays and is publicly available on the above webpage that also includes a detailed user manual. The imple-

216 mentation of pseudo-observables in electroweak Higgs boson production including NLO QCD corrections is underway
217 and will be available at the same Internet link. We have implemented into FEYNRULES [89] (version 2.3.1) a HIGGSPO
218 model, whose source file is named HPO.fr, by means of an effective Lagrangian generating the corresponding vertices at
219 the tree level. We stress that such a Lagrangian should not be considered as a specific model or an effective field theory
220 description, but rather as an auxiliary tool to be used (at tree level only) in order to reproduce the correct Higgs decay
221 amplitude decomposition in terms of pseudo-observables that is valid beyond the tree level.

222 The HIGGSPO FEYNRULES model as implemented in the HPO.fr file is exported to the Universal FeynRules Output
223 (UFO) format [90], which can then be used within the MADGRAPH5_aMC@NLO [91] and SHERPA [92] event gen-
224 erators. The general idea is that after simulating Higgs boson production with a dedicated Monte Carlo generator, the
225 Higgs boson can be decayed at the parton-level with the HIGGSPO model and the partonic events can then be passed to
226 a general purpose event generator for subsequent parton showering and hadronization (such as PYTHIA [93]). This last
227 step will automatically account for the important radiative corrections [88]. We note that it is very practical to use the
228 MADSPIN module [94] of MADGRAPH5_aMC@NLO to decay the Higgs boson with the HIGGSPO model on the fly.
229 We stress again that our FEYNRULES implementation only consists of a set of effective interactions that generate exactly
230 the scattering amplitude of interest at the tree level and is supposed to be used for this purpose only. It should not be used
231 as a Lagrangian for arbitrary process and beyond the tree level.

232 Here we summarize all the Higgs decay processes implemented in the HIGGSPO model, together with the associated
233 Higgs pseudo-observables accessible in the parameter card. The Higgs pseudo-observables relevant for describing the
234 Higgs decays into two fermions are shown in Table 1. The coupling strengths have been assigned an interaction order
235 $YUK = 1$. The pseudo-observables relevant for all other Higgs decays are presented in Table 2 and the coupling strengths
236 have been related to an interaction order $HPO = 1$. Translation of the pseudo-observable language to the Higgs basis
237 defined in Chapter (Ref. to the WG2 chapter) is also available in Refs. [85, 86].

238 1.6 Higgs and Beyond the Standard Model Characterisation in the MADGRAPH5_aMC@NLO Framework

239 The HIGGS CHARACTERISATION (HC) implementation provides a complete framework, based on an effective field
240 theory description, that allows for the study of the Higgs boson properties in a consistent, systematic and accurate way.
241 The HC [95] follows the general strategy outlined in Ref. [96], and has been implemented in a complete simulation chain
242 from Lagrangian to hadron-level events, especially in the FEYNRULES/MADGRAPH5_aMC@NLO framework. The
243 HC effective Lagrangian features bosons $X(J^P)$ with various spin-parity assignments ($J^P = 0^+, 0^-, 1^+, 1^-$ and 2^+)
244 and has been implemented in terms of the Standard Model mass eigenstates into FEYNRULES [89], whose output files are
245 interfaced with various event generators [90, 97]. All model files are publicly available online,

246 <http://feynrules.irmp.ucl.ac.be/wiki/HiggsCharacterisation>.

247 Later on, the HC framework has been extended as a BEYOND THE STANDARD MODEL CHARACTERISATION
248 (BSMC) framework [98] where the effective Lagrangian has been constructed as above, but starting from the Higgs
249 basis Lagrangian (Ref. to the WG2 chapter) where all possible effective operators of dimension up to six are written in
250 terms of the Standard Model mass eigenstates. In particular, fermionic operators different from the Yukawa interactions
251 are now included. However, instead of imposing the realization of the electroweak symmetry that relates the Wilson
252 coefficients, the latter have been kept independent. Due to the lack of manifest $SU(2)_L \times U(1)_Y$ invariance, the BSMC
253 Lagrangian is associated with a larger number of independent coefficients compared to more traditional bases such as the
254 Warsaw [99] or SILH [71, 100] bases. As for the HC case, the BSMC Lagrangian has been implemented into FEYNRULES
255 and is available online,

256 <http://feynrules.irmp.ucl.ac.be/wiki/BSMCharacterisation>.

257 A corresponding implementation of the dimension-six Lagrangian above the weak scale, where $SU(2)_L \times U(1)_Y$ is an
258 exact symmetry, has been also achieved [101] and has overlapping as well as complementary features with respect to the
259 HC and BSMC Lagrangians. It is available at

260 <http://feynrules.irmp.ucl.ac.be/wiki/HEL>.

261 There are several advantages in having a first principle implementation in terms of an effective Lagrangian which can
262 be automatically interfaced to event generators. First and most important, all relevant production and decay modes can
263 be studied within the same model, and the corresponding processes automatically generated within minutes. Second, it is
264 straightforward to modify the model implementation to extend it further in case of need, by adding further interactions, for
265 example of higher-dimensions in energy. Finally, higher-order effects can be easily accounted for, by generating multi-jet
266 merged samples or computing NLO corrections within automatic frameworks. As accumulated data has been increasing,
267 the last point became more and more important. The detailed demonstrations and analyses for all the main production
268 modes of the Higgs boson (gluon fusion, vector boson fusion, Vh associated production and $t\bar{t}h$ production) as well as
269 th production at NLO accuracy in QCD have been done recently [102–104], within the MADGRAPH5_aMC@NLO
270 program [91]. In the following, we focus, for the sake of the example, on a spin-0 (Higgs) boson that is denoted by X_0 ,
271 and compute several differential distributions for some production processes and for different benchmark scenarios.

Scenario	HC parameter choice	Scenario	HC parameter choice
$0^+(\text{GF, SM})$	$\kappa_{Hgg/Htt} = 1 (c_\alpha = 1)$	$0^+(\text{VBF,SM})$	$\kappa_{SM} = 1 (c_\alpha = 1)$
$0^-(\text{GF})$	$\kappa_{A_{gg}/A_{tt}} = 1 (c_\alpha = 0)$	$0^+(\text{VBF,HD})$	$\kappa_{HZZ,HWW} = 1 (c_\alpha = 1)$
$0^\pm(\text{GF})$	$\kappa_{Hgg,A_{gg}/Htt,Att} = 1 (c_\alpha = 1/\sqrt{2})$	$0^-(\text{VBF,HD})$	$\kappa_{AZZ,AWW} = 1 (c_\alpha = 0)$
		$0^\pm(\text{VBF,HD})$	$\kappa_{HZZ,HWW,AZZ,AWW} = 1 (c_\alpha = 1/\sqrt{2})$

Table 3: Benchmark scenarios for X_0 production in the gluon fusion and $t\bar{t}X_0$ (GF) and in the vector boson fusion (VBF) channel.

272 In the HC framework, this means that the only assumptions are that the 125 GeV resonance found at the LHC corre-
273 sponds to a spin-0 state, that no other new state coupled to such a resonance exists below the cutoff scale Λ and that new
274 physics is dominantly described by the lowest dimensional operators. We thus include all effects stemming from the complete
275 set of dimension-six operators allowed by the Standard Model gauge symmetry. The effective interaction Lagrangian
276 is given by

$$\begin{aligned}
\mathcal{L}_0 = & \left\{ - \sum_{f=t,b,\tau} \bar{\psi}_f (c_\alpha \kappa_{Htt} g_{Htt} + i s_\alpha \kappa_{Att} g_{Att} \gamma_5) \psi_f + c_\alpha \kappa_{SM} \left[\frac{1}{2} g_{HZZ} Z_\mu Z^\mu + g_{HWW} W_\mu^+ W^{-\mu} \right] \right. \\
& - \frac{1}{4} [c_\alpha \kappa_{H\gamma\gamma} g_{H\gamma\gamma} A_{\mu\nu} A^{\mu\nu} + s_\alpha \kappa_{A\gamma\gamma} g_{A\gamma\gamma} A_{\mu\nu} \tilde{A}^{\mu\nu}] - \frac{1}{2} [c_\alpha \kappa_{HZ\gamma} g_{HZ\gamma} Z_{\mu\nu} A^{\mu\nu} + s_\alpha \kappa_{AZ\gamma} g_{AZ\gamma} Z_{\mu\nu} \tilde{A}^{\mu\nu}] \\
& - \frac{1}{4} [c_\alpha \kappa_{Hgg} g_{Hgg} G_{\mu\nu}^a G^{a,\mu\nu} + s_\alpha \kappa_{A_{gg}} g_{A_{gg}} G_{\mu\nu}^a \tilde{G}^{a,\mu\nu}] - \frac{1}{4} \frac{1}{\Lambda} [c_\alpha \kappa_{HZZ} Z_{\mu\nu} Z^{\mu\nu} + s_\alpha \kappa_{AZZ} Z_{\mu\nu} \tilde{Z}^{\mu\nu}] \\
& - \frac{1}{2} \frac{1}{\Lambda} [c_\alpha \kappa_{HWW} W_{\mu\nu}^+ W^{-\mu\nu} + s_\alpha \kappa_{AWW} W_{\mu\nu}^+ \tilde{W}^{-\mu\nu}] \\
& \left. - \frac{1}{\Lambda} \kappa_\alpha [\kappa_{H\partial\gamma} Z_\nu \partial_\mu A^{\mu\nu} + \kappa_{H\partial Z} Z_\nu \partial_\mu Z^{\mu\nu} + \kappa_{H\partial W} (W_\nu^+ \partial_\mu W^{-\mu\nu} + h.c.)] \right\} X_0, \quad (28)
\end{aligned}$$

277 where $A_{\mu\nu}$ ($\tilde{A}_{\mu\nu}$), $Z_{\mu\nu}$ ($\tilde{Z}_{\mu\nu}$) and $W_{\mu\nu}^\pm$ ($\tilde{W}_{\mu\nu}^\pm$) represent the reduced field strength tensors of the physical electroweak
278 bosons, and $G_{\mu\nu}^a$ and $\tilde{G}_{\mu\nu}^a$ the gluon field strength tensor and its dual. This parameterization allows for the easy recovery
279 of the Standard Model case by fixing the dimensionless parameters κ_i to appropriate values, since the dimensionful
280 couplings $g_{x_{yy}'}$ are set to their Standard Model values. For instance, we enforce that $g_{H\gamma\gamma} = 47\alpha/18\pi$ and $g_{A_{gg}} = \alpha_s/2\pi$.
281 Moreover, the model description includes the interactions of a 0^- state typical of supersymmetric or of generic theories
282 with two Higgs doublets, and enables the CP -mixing between the 0^+ and 0^- states via a mixing angle α whose sine and
283 cosine are denoted by s_α and c_α . In the Standard Model, $c_\alpha = 1$ and $s_\alpha = 0$.

284 We then make use of MADGRAPH5_AMC@NLO to generate both a numerical code and events, at the NLO accuracy
285 in QCD, for the production of an X_0 state plus two jets in the gluon fusion channel automatically. This is achieved by
286 issuing the following commands (with the / t syntax forbidding diagrams containing top loops),

```

287 > import model HC_NLO_X0-heft
288 > generate p p > x0 j j / t [QCD]
289 > output
290 > launch

```

291 where the -heft suffix in the model name refers to the corresponding model restriction. As a result, all the amplitudes
292 featuring the Higgs-gluon effective vertices in the heavy-top limit are generated, including corrections up to the NLO in
293 QCD. Analogous commands can be issued to generate events related to the production of an X_0 state plus zero and one jet.
294 After the launch command, one can modify the param_card.dat file to change the values of the Λ , κ and c_α parameters.
295 Similarly, a code and events can be generated in the vector boson fusion case (left, with the \$\$ sign forbidding diagrams
296 with W^\pm or Z bosons in the s -channel as they are included in Vh production) and in the VX_0 associated production
297 mode (right) by typing in

```

298 > import model HC_NLO_X0
299 > generate p p > x0 j j $$ w+ w- z / a [QCD]
300 > generate p p > x0 l+ v1 [QCD]
300 > add process p p > x0 l- v1~ [QCD]
300 > add process p p > x0 l+ l- / a [QCD]

```

301 as well as in the $t\bar{t}X_0$ production mode with the command

```

302 > generate p p > x0 t t~ [QCD]

```

303 Furthermore, the X_0 and the top quark decays are subsequently performed starting from the event files generated as above
304 with the help of the MADSPIN [94] package, following the procedure described in Ref. [105] and that allows one to keep
305 spin correlations.

306 We show in Figure 1 (left and central panels) a few kinematical distributions, including theoretical uncertainties, for
307 the benchmark scenarios presented in Table 3. The parton densities are evaluated by using the NNPDF2.3 (LO/NLO)

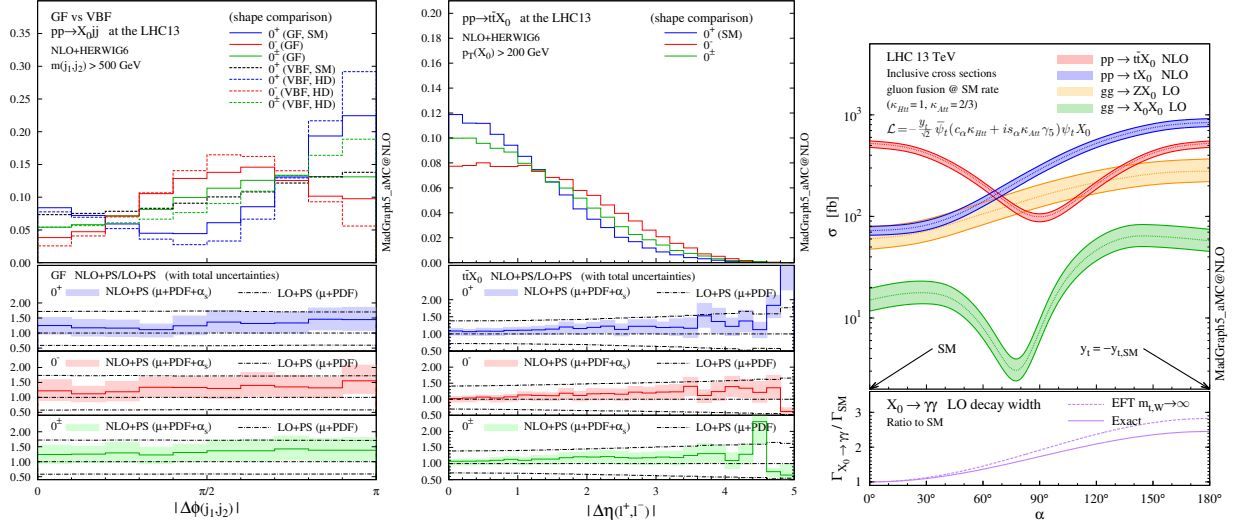


Fig. 1: Normalized kinematical distributions at the LHC, running at a center-of-mass energy of 13 TeV. We show the azimuthal difference between the two tagging jets for $pp \rightarrow X_0jj$ after imposing a $m_{jj} > 500$ GeV selection (left) and the opening angle between the leptons (center) for the dileptonic decay channel in $pp \rightarrow t\bar{t}X_0$ after enforcing a $p_T(X_0) > 200$ GeV selection. For each scenario, the bottom panels give the ratio of the NLO results matched to parton showers to the LO results matched to parton showers, together with the total theoretical uncertainties. In the right panel of the figure, we show NLO (or loop-induced LO) cross sections, presented with the associated scale uncertainties, for $t\bar{t}X_0$ and t -channel tX_0 (ZX_0 and X_0X_0) production as a function of the CP -mixing angle α . The κ_{Htt} and κ_{Att} parameters have been set to reproduce the Standard Model gluon-fusion cross section for every value of α . The ratio of the $X_0 \rightarrow \gamma\gamma$ partial decay width to the corresponding Standard Model value is also shown in the lower panel of the figure.

parameterization [106] and the central value μ_0 for the renormalization (μ_R) and factorisation (μ_F) scales is set to $H_T/2$, m_W and $\sqrt[3]{m_T(t)m_T(\bar{t})m_T(X_0)}$ in the gluon fusion, vector boson fusion and $t\bar{t}X_0$ production channel respectively. Uncertainties coming from missing higher orders are estimated by varying μ_R and μ_F independently by a factor of two up and down around μ_0 . Finally, in the right panel of the figure, we present the dependence of the th and $t\bar{t}X_0$ production cross sections on the CP -mixing angle α . The nature of the top quark Yukawa coupling also affects the loop-induced Higgs coupling to gluons and photons. In order to maintain the Standard Model gluon-fusion production cross section, the rescaling parameters are set to $\kappa_{Htt} = 1$ and $\kappa_{Att} = 2/3$. The LO cross sections for the loop-induced HZ [107] and HH [108] production processes via gluon fusion are also shown as references.

1.7 Anomalous Couplings in VBFNLO

Next-to-leading order QCD predictions including anomalous couplings effects can be studied for several processes with the flexible Monte Carlo program VBFNLO [109, 110], available at

<https://www.itp.kit.edu/vbfnlo>.

The ensemble of implemented processes includes Higgs, single and double vector boson production via vector boson fusion (VBF), WH production, as well as double and triple vector boson (plus jet) production. The Standard Model QCD-induced background for double vector boson production in association with two jets is also available at the NLO accuracy. Furthermore, anomalous HVV coupling effects are also included in the gluon-induced contributions to diboson (plus jet) production as well as in the gluon fusion processes $gg \rightarrow Hjj \rightarrow VVjj$. Although these processes are all one-loop induced and hence computed at the leading-order accuracy, the full top- and bottom-quark mass dependence is retained.

In the VBFNLO-3.0 β release, an interface compliant with the Binoth Les Houches Accord (BLHA) [111, 112] has been added for all VBF processes including fully leptonic decays, which allows for Monte Carlo studies at NLO in QCD including the full functionality of event generators like HERWIG 7 [113, 114]. The K -matrix unitarization procedure has been implemented for the two dimension-eight operators $\mathcal{O}_{S,0} + \mathcal{O}_{S,2}$ and $\mathcal{O}_{S,1}$ that are defined in Eq. (32) below. The strength of the anomalous triple and quartic gauge boson couplings can be set in the file `anomV.dat`. They are parameterized using an effective Lagrangian, as described in Refs. [115–118],

$$\mathcal{L}_{\text{eff}} = \sum_i \frac{f_i}{\Lambda^n} \mathcal{O}_i^{n+4}, \quad (29)$$

where $n + 4$ signifies the dimension of the operator \mathcal{O}_i . VBFNLO then defines anomalous gauge couplings in terms of

334 the coefficients f_i/Λ^n of the dimension-six and dimension-eight operators. The full list of implemented operators can
 335 be found in the Appendix 1 of the VBFNLO manual [119]. The explicit form of the included \mathcal{CP} -even dimension-six
 336 operators is given by

$$\begin{aligned}\mathcal{O}_W &= (D_\mu\Phi)^\dagger \widehat{W}^{\mu\nu} (D_\nu\Phi), & \mathcal{O}_B &= (D_\mu\Phi)^\dagger \widehat{B}^{\mu\nu} (D_\nu\Phi), & \mathcal{O}_{WWW} &= \text{Tr} \left[\widehat{W}_{\mu\nu} \widehat{W}^{\nu\rho} \widehat{W}_\rho{}^\mu \right], \\ \mathcal{O}_{WW} &= \Phi^\dagger \widehat{W}_{\mu\nu} \widehat{W}^{\mu\nu} \Phi, & \mathcal{O}_{BB} &= \Phi^\dagger \widehat{B}_{\mu\nu} \widehat{B}^{\mu\nu} \Phi.\end{aligned}\quad (30)$$

337 The building blocks for these operators (following the notation of Refs. [116, 120]) are defined by

$$\widehat{W}_{\mu\nu} = igT_a W_{\mu\nu}^a, \quad \widehat{B}_{\mu\nu} = ig'Y B_{\mu\nu}, \quad D_\mu = \partial_\mu + igT_a W_\mu^a + ig'Y B_\mu, \quad (31)$$

338 where g and g' are the $SU(2)_L$ and $U(1)_Y$ gauge couplings, and T_a and Y the generators of the $SU(2)$ group in the
 339 fundamental representation and the hypercharge operator, respectively. The \mathcal{CP} -odd part of the Lagrangian is obtained
 340 replacing the field strength tensor with the corresponding dual field strength tensors. The dimension-eight operators
 341 that are supported are taken from Ref. [117] although slightly different normalizations for the field strength tensors are
 342 employed in this work, $\widehat{W}_{\mu\nu} = T_a W_{\mu\nu}^a$ and $\widehat{B}_{\mu\nu} = B_{\mu\nu}$. The conversion factors for the coupling strengths f_i relating
 343 Ref. [117] to our implementation can be found in the Appendix 1 of the VBFNLO manual. The dimension-eight operators
 344 that are supported can be split into three categories, namely operators depending on the gauge-covariant derivative $D_\mu\Phi$
 345 only,

$$\begin{aligned}\mathcal{O}_{S,0} &= \left[(D_\mu\Phi)^\dagger D_\nu\Phi \right] \left[(D^\mu\Phi)^\dagger D^\nu\Phi \right], & \mathcal{O}_{S,1} &= \left[(D_\mu\Phi)^\dagger D^\mu\Phi \right] \left[(D_\nu\Phi)^\dagger D^\nu\Phi \right], \\ \mathcal{O}_{S,2} &= \left[(D_\mu\Phi)^\dagger D_\nu\Phi \right] \left[(D^\nu\Phi)^\dagger D^\mu\Phi \right],\end{aligned}\quad (32)$$

346 operators depending on both $D_\mu\Phi$ and the electroweak field strength tensors $\widehat{W}_{\mu\nu}$ and $\widehat{B}_{\mu\nu}$, e.g.,

$$\mathcal{L}_{M,0} = \text{Tr} \left[\widehat{W}_{\mu\nu} \widehat{W}^{\mu\nu} \right] \left[(D_\rho\Phi)^\dagger D^\rho\Phi \right], \quad (33)$$

347 and operators depending only on the electroweak field strength tensors $\widehat{W}_{\mu\nu}$ and $\widehat{B}_{\mu\nu}$, such as,

$$\mathcal{L}_{T,0} = \text{Tr} \left[\widehat{W}_{\mu\nu} \widehat{W}^{\mu\nu} \right] \text{Tr} \left[\widehat{W}_{\rho\sigma} \widehat{W}^{\rho\sigma} \right]. \quad (34)$$

348 Anomalous Higgs boson HVV coupling parameters are controlled in VBFNLO via the file `anom_HVV.dat`, where
 349 three different parameterizations are available. The latter consist of the Wilson coefficients associated with the subset
 350 of dimension-six operators introduced above that contribute to the Higgs couplings, the parametrization used by the L3
 351 collaboration that is defined in Ref. [121], and a parameterization based on anomalous couplings in the mass basis that is
 352 thus expressed in terms of the field strength and dual field strength tensors of the W and Z bosons [122]. The relationships
 353 between these three parameterizations are discussed in more detail on the VBFNLO webpage.

354 Since the pure operators for anomalous gauge boson couplings might lead to a violation of tree-level unitarity within
 355 the energy range of the LHC, special care has to be taken to avoid this unphysical behaviour. Within VBFNLO, we have
 356 opted for using the following form factors, all of them depending on Λ , the characteristic scale where the form factor
 357 effects become relevant. Equivalently, introducing these form factors is like restricting the validity range of the effective
 358 field theory rather than implementing a sharp cutoff. For HVV vertices, two different form factors can be chosen as
 359 described in Refs. [122, 123].

$$F_1 = \frac{\Lambda^2}{|q_1|^2 + \Lambda^2} \frac{\Lambda^2}{|q_2|^2 + \Lambda^2}, \quad F_2 = -2\Lambda^2 C_0(q_1^2, q_2^2, (q_1 + q_2)^2, \Lambda^2). \quad (35)$$

360 where q_i are the momenta of the vector bosons and C_0 is the scalar one-loop three point function in the notation of
 361 Ref. [124]. For triple and quartic gauge couplings the form factor takes the form

$$F = \left(1 + \frac{s}{\Lambda^2} \right)^{-p}, \quad (36)$$

362 for each phase space point, where s is a universal scale identified with the invariant mass squared of the produced bosons.
 363 Finally, for γjj production in VBF, the form factor reads

$$F = \left(1 + \frac{|q_1|^2}{\Lambda^2} + \frac{|q_2|^2}{\Lambda^2} + \frac{|q_3|^2}{\Lambda^2} \right)^{-p}, \quad (37)$$

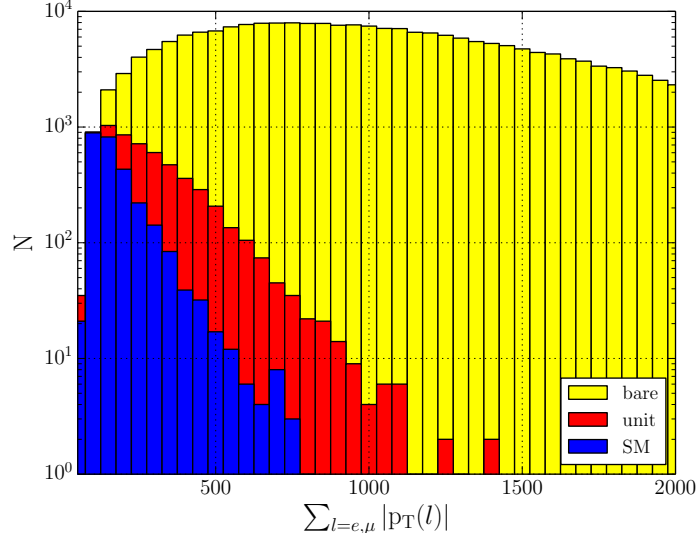


Fig. 2: Events generated by WHIZARD when a dimension-eight coupling $F_{S,0} = 480 \text{ TeV}^{-4}$ (the Wilson coefficient associated with the $\mathcal{O}_{S,0}$ operator of Eq. (32)) is added to the Standard Model and for the process $pp \rightarrow e^+ \mu^+ \nu_e \nu_\mu jj$ at a center-of-mass energy of 14 TeV and for an integrated luminosity of $\mathcal{L} = 1000 \text{ fb}^{-1}$. Event selection requires a dijet invariant mass $M_{jj} > 500 \text{ GeV}$, a rapidity separation between the jets of $\Delta y_{jj} > 2.4$, and the two jets must have a transverse momentum $p_T^j > 20 \text{ GeV}$ and a pseudorapidity $|\eta_j| < 4.5$. In addition, leptons are required to have a transverse momentum $p_T^l > 20 \text{ GeV}$. Red and yellow histograms represent the naive and unitarized effective field theory predictions, respectively, while the pure Standard model expectation is shown as a blue histogram for comparison.

364 with q_1^2 , q_2^2 and q_3^2 as the invariant masses squared of the three vector bosons involved in the VVV vertex. On the VBFNLO
 365 webpage, we provide the ‘Formfactor Calculation Tool for aGC’ which gives the maximum value of the scale Λ which
 366 is allowed by unitarity. The value is determined by calculating on-shell VV scattering and computing the zeroth partial
 367 wave of the amplitude. As unitarity criterion, the absolute value of the real part of the zeroth partial wave has to be
 368 below 0.5 [125]. Each channel in $VV \rightarrow VV$ scattering (with $V = W/Z/\gamma$) is checked individually, while additionally
 369 channels with the same electrical charge for the VV system are combined [126]. We recall that the definition of the partial
 370 wave expansion in Ref. [126] differs from ours by a factor of 2.

371 Finally, the K -matrix unitarization procedure has been implemented for the two dimension-eight operators $\mathcal{O}_{S,0} + \mathcal{O}_{S,2}$
 372 and $\mathcal{O}_{S,1}$ by using the relations to the operators \mathcal{O}_4 and \mathcal{O}_5 of the electroweak chiral Lagrangian and the procedure worked
 373 out in Ref. [127]. This method guarantees the preservation of unitarity when either of these operators is used in the study
 374 of anomalous quartic gauge couplings. In contrast to using form factors, no additional input parameters need to be set.
 375 The anomalous contributions are automatically suppressed at the energy scale where unitarity would be violated without
 376 unitarization. After this energy scale is reached, the anomalous contributions are kept at a finite value, representing the
 377 maximally possible anomalous contribution. We refer to Refs. [118, 127, 128] for details of the K -matrix unitarization
 378 procedure and its implementation.

379 1.8 Event generation with WHIZARD

380 WHIZARD [129] is a multipurpose event generator for hadron and lepton colliders. It has a highly optimized internal matrix
 381 element generator, O’MEGA, for the recursive computing of tree-level amplitudes for almost arbitrary theories [130].
 382 In the QCD case, it additionally uses the color flow formalism [131]. WHIZARD has its own parton shower implementation
 383 [132], with both a p_T -ordered shower and an analytic shower. Recently, automated FKS subtraction and POWHEG
 384 matching for NLO QCD corrections (using external virtual matrix elements) have been implemented [133, 134]. For external
 385 theories beyond the Standard Model, interfaces to the packages SARAH and FEYNRULES [135] are available, and
 386 support for the UFO file format allowing for arbitrary Lorentz and color structures is currently under way.

387 With respect to Higgs Effective Field Theories and higher-dimensional operators, WHIZARD supports the whole set
 388 of bosonic dimension-six operators in the Warsaw basis [99]. For vector-boson scattering at the LHC, usually dimension-
 389 eight operators in the coupled system of electroweak gauge and Higgs bosons are as important as dimension-six operators
 390 as they can be generated at tree-level in some new physics models. These electroweak dimension-eight operators have been
 391 implemented in WHIZARD, both as plain operators and also with their interplay with new resonances in the electroweak
 392 sector. The description of new physics contributions with a low energy effective energy is however only valid up to an

393 a priori unknown scale Λ . At energies above Λ , the effective field theory will lead to unphysical predictions. As an
394 example, the sum of the norm of the transverse momenta of all leptons produced in the process $pp \rightarrow e^+ \mu^+ \nu_e \nu_\mu$ is shown
395 on Figure 2 when the dimension-eight operator $\mathcal{O}_{S,0}$ of Eq. (32) is included. The number of events generated with a naive
396 effective field theory description (yellow histogram) will largely overshoot a physically possible distribution, because S -
397 matrix unitarity is violated within the experimental energy reach. A selection to avoid energy regions where the theoretical
398 description breaks down is not possible in general, due to the inability to reconstruct the invariant mass for some final
399 states. Using the T -matrix scheme, a unitarization prescription for high-energy regions of the phase space [127, 128, 136],
400 avoid the unphysical high number of generated events by WHIZARD. Instead, the number of events are saturated in every
401 isospin-spin channel to satisfy S -matrix unitarity (red histogram). In order to simplify unitarization, WHIZARD does not
402 use the basis of Ref. [137] as this basis does not respect isospin symmetry which makes calculation of the channels in
403 need for unitarization much easier.

404 On different lines, fermionic dimension-six operators are implemented for the top quark sector as (form-factor regu-
405 larized) anomalous couplings [138, 139].

406 1.9 ROSETTA

407 Different complete and non-redundant operator bases of dimension-six effective operators have been proposed in the
408 literature, the most popular choices including the Warsaw basis [99], the SILH basis [71, 100] and the beyond the Standard
409 Model primaries basis [140–142]. It is however cumbersome to express any experimental result in a basis-independent
410 manner. Different bases may be convenient for particular applications, either because they facilitate the comparison with
411 a given class of theories or simply because different experimental analyses look more transparent in a specific basis. The
412 ROSETTA package [98] has been designed to explicitly solve such problems by allowing for a straightforward translation
413 between different effective field theory languages. In addition to translating, another important goal of the ROSETTA
414 program is to provide a platform for communication with Monte Carlo event generators, no matter which basis is chosen.
415 To achieve this, ROSETTA contains an implementation of the Higgs basis (Ref. to the WG2 chapter) and is connected to
416 the BSMC Lagrangian introduced in Section 1.6. More precisely, the output format of ROSETTA has been tuned so that the
417 translation maps an effective field theory Lagrangian given in a specific basis to the BSMC Lagrangian and generates an
418 output file that is compatible with the BSMC implementation into FEYNRULES [89]. As a consequence, any high-energy
419 physics tool that is interfaced to FEYNRULES can be employed within the context of any basis of dimension-six operators
420 that is included in ROSETTA. A full description of the program including detailed example usage and information on how
421 to create a user-defined basis class can be found in the manual [98].

422 The most basic functionality of ROSETTA is to map a chosen set of input parameters (the Wilson coefficients in a
423 specific basis choice) onto the BSMC coefficients such that the output can be employed within tools relying on a BSMC
424 Lagrangian description. In addition, the user may define his/her own map to the BSMC coefficients (or to any other basis
425 implementation) and proceed with event generation using the related FEYNRULES implementation. This highlights one
426 of the key features of ROSETTA, the possibility to easily define one’s own input basis and directly use it in the context
427 of many programs via the translation functionality. An example of this would be the eHDECAY program (see Ref. [100]
428 and Section 1.4) for which ROSETTA provides an interface to calculate the Higgs width and branching fractions including
429 effective field theory effects in any basis. The strength of this approach is that it is much simpler than developing from
430 scratch new modules for existing tools in the context of a new basis. Moreover, ROSETTA not only enables translation
431 into the BSMC Lagrangian, but also allows for translations into any of the other bases included in the package that are
432 currently the Higgs, Warsaw and SILH bases. Translations between these three bases in any direction are possible, so
433 that the addition of a new basis by the user only requires the specification of translation rules to any one of the three core
434 bases. One is subsequently able to indirectly translate the new basis into any of the other two bases, as well as into the
435 BSMC Lagrangian.

436 The latest release of ROSETTA can be obtained from

437 <http://rosetta.hepforge.org>.

438 The package contains a PYTHON executable named `translate`, an information file named `README` and two directories,
439 a first folder (named `Cards`) collecting example input files and a second folder (named `Rosetta`) including the source
440 code of ROSETTA. Each basis is implemented as a class in its own PYTHON module, where the coefficients and the
441 required inputs are declared. Moreover, the input format must respect conventions inspired by the Supersymmetry Les
442 Houches Accord (SLHA) [143, 144] and the related SLHA block structure is defined in the class. Translations are defined
443 as member functions of the class with a special syntax to identify the target basis. Several utility functions may also be im-
444 plemented to either calculate the values of parameters declared as dependent as a function of those declared as independent
445 or modify the values of the Standard Model input parameters as a function of the effective operator coefficients.

446 The `translate` executable takes as input an SLHA-style parameter file with the coefficients of the dimension-six
447 operators associated with a particular basis. Information on the format of such an input file can be found in the manual [98].
448 Depending on the basis implementation, some basic input quantities, such as Standard Model input constants and particle
449 masses may be required in addition to the effective field theory coefficients. The execution of the `translate` script

450 from a shell yields the generation of an output parameter file where all parameters are this time the coefficients of the
451 dimension-six operators associated with a specified new basis, the default choice being the BSMC Lagrangian. The tool
452 can be used by typing in

```
453 ./translate PARAMCARD.dat OPTION
```

454 where PARAMCARD.dat is the name of the SLHA-style input file and OPTIONS stands for optional arguments. These can
455 range from specifying the output file name (-output, -o) or target basis into which to translate (-target, -t) to invoking
456 the eHDECAY (-ehdecay, -e) interface to additionally generate an SLHA decay block for the Higgs as part of the output
457 file. A particularly useful option is the -flavour or -f one which allows users to specify the treatment of the flavor
458 structure relevant for fermionic operators. This can take the values general, diagonal and universal depending on
459 the desired degree of simplicity. A more complicated example of usage might read

```
460 ./translate myinput.dat -t warsaw -f universal -e -o myoutput.dat
```

461 which would read the myinput.dat file and translate it to the Warsaw basis, assuming the universal flavor structure which
462 is designed to map easily to the Minimal Flavour Violation assumption [145]. The eHDECAY interface will also be called,
463 writing in the output file, specified to be myoutput.dat an additional SLHA block containing Higgs decay information.

464 With the advent of NLO-accurate Monte Carlo event generation software, it is important that ROSETTA remains
465 flexible enough to eventually provide compatibility with this new generation of tools. The future development plans of
466 the program are connected to the recent progresses that have been made on the theory side both in implementing the linear
467 dimension-six description in the FEYNRULES framework [146] and in calculating the renormalization group evolution
468 of the full set of operators and their mutual mixing [147–150]. In the former case, ROSETTA can simply be extended to
469 provide an output compatible with the eventual NLO model implementation, analogously to the BSMC Lagrangian. The
470 latter case of evaluating the renormalization group running effects, while being a slightly separate issue, highlights a key
471 feature of ROSETTA, given that the calculation of these effects has only been performed in the Warsaw basis and that
472 ROSETTA could allow for the application of these results in any desired basis.

473 References

- 474 [1] ATLAS Collaboration, G. Aad *et al.*, Phys.Lett. **B716**, 1 (2012), 1207.7214. (1)
475 [2] CMS Collaboration, S. Chatrchyan *et al.*, Phys.Lett. **B716**, 30 (2012), 1207.7235. (1)
476 [3] M. Spira, (1995), hep-ph/9510347. (1)
477 [4] M. Spira, Nucl. Instrum. Meth. **A389**, 357 (1997), hep-ph/9610350. (1)
478 [5] A. Djouadi, M. Spira, and P. M. Zerwas, Phys. Lett. **B264**, 440 (1991). (1, 5)
479 [6] S. Dawson, Nucl. Phys. **B359**, 283 (1991). (1)
480 [7] D. Graudenz, M. Spira, and P. M. Zerwas, Phys. Rev. Lett. **70**, 1372 (1993). (1)
481 [8] M. Spira, A. Djouadi, D. Graudenz, and P. M. Zerwas, Nucl. Phys. **B453**, 17 (1995), hep-ph/9504378. (1, 5)
482 [9] R. Harlander and P. Kant, JHEP **12**, 015 (2005), hep-ph/0509189. (1)
483 [10] C. Anastasiou, S. Bucherer, and Z. Kunszt, JHEP **10**, 068 (2009), 0907.2362. (1)
484 [11] S. Catani, D. de Florian, and M. Grazzini, JHEP **05**, 025 (2001), hep-ph/0102227. (1)
485 [12] R. V. Harlander and W. B. Kilgore, Phys. Rev. **D64**, 013015 (2001), hep-ph/0102241. (1)
486 [13] R. V. Harlander and W. B. Kilgore, Phys. Rev. Lett. **88**, 201801 (2002), hep-ph/0201206. (1)
487 [14] V. Ravindran, J. Smith, and W. L. van Neerven, Nucl. Phys. **B665**, 325 (2003), hep-ph/0302135. (1)
488 [15] C. Anastasiou and K. Melnikov, Nucl. Phys. **B646**, 220 (2002), hep-ph/0207004. (1)
489 [16] A. Djouadi and P. Gambino, Phys. Rev. Lett. **73**, 2528 (1994), hep-ph/9406432. (1, 5)
490 [17] K. G. Chetyrkin, B. A. Kniehl, and M. Steinhauser, Phys. Rev. Lett. **78**, 594 (1997), hep-ph/9610456. (1, 5)
491 [18] K. G. Chetyrkin, B. A. Kniehl, and M. Steinhauser, Nucl. Phys. **B490**, 19 (1997), hep-ph/9701277. (1, 5)
492 [19] U. Aglietti, R. Bonciani, G. Degrassi, and A. Vicini, Phys. Lett. **B595**, 432 (2004), hep-ph/0404071. (1, 5)
493 [20] U. Aglietti, R. Bonciani, G. Degrassi, and A. Vicini, Two-loop electroweak corrections to Higgs production in
494 proton-proton collisions, in *TeV4LHC Workshop: 2nd Meeting Brookhaven, Upton, New York, February 3-5, 2005*,
495 2006, hep-ph/0610033. (1, 5)
496 [21] G. Degrassi and F. Maltoni, Phys. Lett. **B600**, 255 (2004), hep-ph/0407249. (1, 5)
497 [22] S. Actis, G. Passarino, C. Sturm, and S. Uccirati, Phys. Lett. **B670**, 12 (2008), 0809.1301. (1, 5)
498 [23] S. Actis, G. Passarino, C. Sturm, and S. Uccirati, Nucl. Phys. **B811**, 182 (2009), 0809.3667. (1, 5)
499 [24] C. Anastasiou, R. Boughezal, and F. Petriello, JHEP **04**, 003 (2009), 0811.3458. (1)
500 [25] R. P. Kauffman and W. Schaffer, Phys. Rev. **D49**, 551 (1994), hep-ph/9305279. (1)
501 [26] A. Djouadi, M. Spira, and P. M. Zerwas, Phys. Lett. **B311**, 255 (1993), hep-ph/9305335. (1)
502 [27] M. Spira, A. Djouadi, D. Graudenz, and P. M. Zerwas, Phys. Lett. **B318**, 347 (1993). (1)

- 503 [28] S. Dawson, A. Djouadi, and M. Spira, *Phys. Rev. Lett.* **77**, 16 (1996), hep-ph/9603423. (1)
- 504 [29] M. Muhlleitner and M. Spira, *Nucl. Phys.* **B790**, 1 (2008), hep-ph/0612254. (1)
- 505 [30] R. Bonciani, G. Degrassi, and A. Vicini, *JHEP* **11**, 095 (2007), 0709.4227. (1)
- 506 [31] C. Anastasiou, S. Beerli, S. Bucherer, A. Daleo, and Z. Kunszt, *JHEP* **01**, 082 (2007), hep-ph/0611236. (1)
- 507 [32] U. Aglietti, R. Bonciani, G. Degrassi, and A. Vicini, *JHEP* **01**, 021 (2007), hep-ph/0611266. (1)
- 508 [33] R. V. Harlander and W. B. Kilgore, *JHEP* **10**, 017 (2002), hep-ph/0208096. (1)
- 509 [34] C. Anastasiou and K. Melnikov, *Phys. Rev.* **D67**, 037501 (2003), hep-ph/0208115. (1)
- 510 [35] R. V. Harlander and M. Steinhauser, *Phys. Lett.* **B574**, 258 (2003), hep-ph/0307346. (1)
- 511 [36] R. Harlander and M. Steinhauser, *Phys. Rev.* **D68**, 111701 (2003), hep-ph/0308210. (1)
- 512 [37] R. V. Harlander and M. Steinhauser, *JHEP* **09**, 066 (2004), hep-ph/0409010. (1)
- 513 [38] R. V. Harlander and F. Hofmann, *JHEP* **03**, 050 (2006), hep-ph/0507041. (1)
- 514 [39] G. Degrassi and P. Slavich, *Nucl. Phys.* **B805**, 267 (2008), 0806.1495. (1)
- 515 [40] G. Degrassi and P. Slavich, *JHEP* **11**, 044 (2010), 1007.3465. (1)
- 516 [41] G. Degrassi, S. Di Vita, and P. Slavich, *JHEP* **08**, 128 (2011), 1107.0914. (1)
- 517 [42] G. Degrassi, S. Di Vita, and P. Slavich, *Eur. Phys. J.* **C72**, 2032 (2012), 1204.1016. (1)
- 518 [43] C. Anastasiou, S. Beerli, and A. Daleo, *Phys. Rev. Lett.* **100**, 241806 (2008), 0803.3065. (1)
- 519 [44] M. Muhlleitner, H. Rzehak, and M. Spira, *PoS RADCOR2009*, 043 (2010), 1001.3214, [42(2010)]. (1)
- 520 [45] M. Muhlleitner, H. Rzehak, and M. Spira, MSSM Higgs boson production via gluon fusion, in *Physics at the*
521 *LHC2010. Proceedings, 5th Conference, PLHC2010, Hamburg, Germany, June 7-12, 2010*, pp. 415–417, 2010.
522 (1)
- 523 [46] K. G. Chetyrkin, B. A. Kniehl, and M. Steinhauser, *Phys. Rev. Lett.* **79**, 2184 (1997), hep-ph/9706430. (1)
- 524 [47] K. G. Chetyrkin, B. A. Kniehl, and M. Steinhauser, *Nucl. Phys.* **B510**, 61 (1998), hep-ph/9708255. (1, 5)
- 525 [48] M. Kramer, E. Laenen, and M. Spira, *Nucl. Phys.* **B511**, 523 (1998), hep-ph/9611272. (1, 5)
- 526 [49] M. Spira, *Fortsch. Phys.* **46**, 203 (1998), hep-ph/9705337. (1)
- 527 [50] D. Choudhury and P. Saha, *JHEP* **08**, 144 (2012), 1201.4130. (1)
- 528 [51] C. Degrande, J. M. Gerard, C. Grojean, F. Maltoni, and G. Servant, *JHEP* **07**, 036 (2012), 1205.1065, [Erratum:
529 *JHEP03,032(2013)*]. (1)
- 530 [52] C. G. Callan, Jr., *Phys. Rev.* **D2**, 1541 (1970). (2)
- 531 [53] K. Symanzik, *Commun. Math. Phys.* **18**, 227 (1970). (2)
- 532 [54] S. R. Coleman and R. Jackiw, *Annals Phys.* **67**, 552 (1971). (2)
- 533 [55] R. J. Crewther, *Phys. Rev. Lett.* **28**, 1421 (1972). (2)
- 534 [56] M. S. Chanowitz and J. R. Ellis, *Phys. Lett.* **B40**, 397 (1972). (2)
- 535 [57] M. S. Chanowitz and J. R. Ellis, *Phys. Rev.* **D7**, 2490 (1973). (2)
- 536 [58] A. Djouadi, J. Kalinowski, and M. Spira, *Comput. Phys. Commun.* **108**, 56 (1998), hep-ph/9704448. (2, 4)
- 537 [59] A. Djouadi, M. M. Muhlleitner, and M. Spira, *Acta Phys. Polon.* **B38**, 635 (2007), hep-ph/0609292. (2, 4)
- 538 [60] S. Dawson, S. Dittmaier, and M. Spira, *Phys. Rev.* **D58**, 115012 (1998), hep-ph/9805244. (3)
- 539 [61] J. Grigo, J. Hoff, K. Melnikov, and M. Steinhauser, *Nucl. Phys.* **B875**, 1 (2013), 1305.7340. (3)
- 540 [62] R. Frederix *et al.*, *Phys. Lett.* **B732**, 142 (2014), 1401.7340. (3)
- 541 [63] F. Maltoni, E. Vryonidou, and M. Zaro, *JHEP* **11**, 079 (2014), 1408.6542. (3)
- 542 [64] J. Grigo, J. Hoff, and M. Steinhauser, *Nucl. Phys.* **B900**, 412 (2015), 1508.00909. (3)
- 543 [65] D. de Florian and J. Mazzitelli, *Phys. Rev. Lett.* **111**, 201801 (2013), 1309.6594. (3)
- 544 [66] D. de Florian and J. Mazzitelli, *JHEP* **09**, 053 (2015), 1505.07122. (3)
- 545 [67] J. Grigo, K. Melnikov, and M. Steinhauser, *Nucl. Phys.* **B888**, 17 (2014), 1408.2422. (3)
- 546 [68] R. Grober, M. Muhlleitner, M. Spira, and J. Streicher, *JHEP* **09**, 092 (2015), 1504.06577. (3)
- 547 [69] E. W. N. Glover and J. J. van der Bij, *Nucl. Phys.* **B309**, 282 (1988). (3)
- 548 [70] T. Plehn, M. Spira, and P. M. Zerwas, *Nucl. Phys.* **B479**, 46 (1996), hep-ph/9603205, [Erratum: *Nucl.*
549 *Phys.*B531,655(1998)]. (3)
- 550 [71] G. F. Giudice, C. Grojean, A. Pomarol, and R. Rattazzi, *JHEP* **06**, 045 (2007), hep-ph/0703164. (4, 7, 12)
- 551 [72] R. Contino, M. Ghezzi, C. Grojean, M. Mühlleitner, and M. Spira, *Comput. Phys. Commun.* **185**, 3412 (2014),
552 1403.3381. (4)
- 553 [73] K. Agashe, R. Contino, and A. Pomarol, *Nucl. Phys.* **B719**, 165 (2005), hep-ph/0412089. (4)

- 554 [74] R. Contino, L. Da Rold, and A. Pomarol, Phys. Rev. **D75**, 055014 (2007), hep-ph/0612048. (4)
- 555 [75] Y. Schroder and M. Steinhauser, JHEP **0601**, 051 (2006), hep-ph/0512058. (5)
- 556 [76] K. Chetyrkin, J. H. Kuhn, and C. Sturm, Nucl.Phys. **B744**, 121 (2006), hep-ph/0512060. (5)
- 557 [77] P. Baikov and K. Chetyrkin, Phys.Rev.Lett. **97**, 061803 (2006), hep-ph/0604194. (5)
- 558 [78] T. Inami, T. Kubota, and Y. Okada, Z.Phys. **C18**, 69 (1983). (5)
- 559 [79] K. Chetyrkin, B. A. Kniehl, and M. Steinhauser, Phys.Rev.Lett. **79**, 353 (1997), hep-ph/9705240. (5)
- 560 [80] J. R. Ellis, M. K. Gaillard, and D. V. Nanopoulos, Nucl.Phys. **B106**, 292 (1976). (5)
- 561 [81] M. A. Shifman, A. Vainshtein, M. Voloshin, and V. I. Zakharov, Sov.J.Nucl.Phys. **30**, 711 (1979). (5)
- 562 [82] B. A. Kniehl and M. Spira, Z.Phys. **C69**, 77 (1995), hep-ph/9505225. (5)
- 563 [83] A. Denner *et al.*, Report No. LHCHXSWG-INT-2015-006, 2015 (unpublished). (5)
- 564 [84] LHC Higgs Cross Section Working Group, A. David *et al.*, (2012), 1209.0040. (5)
- 565 [85] M. Gonzalez-Alonso, A. Greljo, G. Isidori, and D. Marzocca, Eur. Phys. J. **C75**, 128 (2015), 1412.6038. (6, 7)
- 566 [86] A. Greljo, G. Isidori, J. M. Lindert, and D. Marzocca, (2015), 1512.06135. (6, 7)
- 567 [87] J. S. Gainer, J. Lykken, K. T. Matchev, S. Mrenna, and M. Park, The Matrix Element Method: Past, Present, and
568 Future, in *Community Summer Study 2013: Snowmass on the Mississippi (CSS2013) Minneapolis, MN, USA, July*
569 *29-August 6, 2013*, 2013, 1307.3546. (6)
- 570 [88] M. Bordone, A. Greljo, G. Isidori, D. Marzocca, and A. Pattori, Eur. Phys. J. **C75**, 385 (2015), 1507.02555. (6, 7)
- 571 [89] A. Alloul, N. D. Christensen, C. Degrande, C. Duhr, and B. Fuks, Comput. Phys. Commun. **185**, 2250 (2014),
572 1310.1921. (7, 12)
- 573 [90] C. Degrande *et al.*, Comput. Phys. Commun. **183**, 1201 (2012), 1108.2040. (7)
- 574 [91] J. Alwall *et al.*, JHEP **07**, 079 (2014), 1405.0301. (7)
- 575 [92] T. Gleisberg *et al.*, JHEP **02**, 007 (2009), 0811.4622. (7)
- 576 [93] T. Sjostrand, S. Mrenna, and P. Z. Skands, Comput. Phys. Commun. **178**, 852 (2008), 0710.3820. (7)
- 577 [94] P. Artoisenet, R. Frederix, O. Mattelaer, and R. Rietkerk, JHEP **03**, 015 (2013), 1212.3460. (7, 8)
- 578 [95] P. Artoisenet *et al.*, JHEP **11**, 043 (2013), 1306.6464. (7)
- 579 [96] N. D. Christensen *et al.*, Eur. Phys. J. **C71**, 1541 (2011), 0906.2474. (7)
- 580 [97] P. de Aquino, W. Link, F. Maltoni, O. Mattelaer, and T. Stelzer, Comput. Phys. Commun. **183**, 2254 (2012),
581 1108.2041. (7)
- 582 [98] A. Falkowski *et al.*, Eur. Phys. J. **C75**, 583 (2015), 1508.05895. (7, 12)
- 583 [99] B. Grzadkowski, M. Iskrzynski, M. Misiak, and J. Rosiek, JHEP **10**, 085 (2010), 1008.4884. (7, 11, 12)
- 584 [100] R. Contino, M. Ghezzi, C. Grojean, M. Mühlleitner, and M. Spira, JHEP **1307**, 035 (2013), 1303.3876. (7, 12)
- 585 [101] A. Alloul, B. Fuks, and V. Sanz, JHEP **04**, 110 (2014), 1310.5150. (7)
- 586 [102] F. Maltoni, K. Mawatari, and M. Zaro, Eur. Phys. J. **C74**, 2710 (2014), 1311.1829. (7)
- 587 [103] F. Demartin, F. Maltoni, K. Mawatari, B. Page, and M. Zaro, Eur. Phys. J. **C74**, 3065 (2014), 1407.5089. (7)
- 588 [104] F. Demartin, F. Maltoni, K. Mawatari, and M. Zaro, Eur. Phys. J. **C75**, 267 (2015), 1504.00611. (7)
- 589 [105] S. Frixione, E. Laenen, P. Motylinski, and B. R. Webber, JHEP **04**, 081 (2007), hep-ph/0702198. (8)
- 590 [106] R. D. Ball *et al.*, Nucl. Phys. **B867**, 244 (2013), 1207.1303. (9)
- 591 [107] B. Hespel, F. Maltoni, and E. Vryonidou, JHEP **06**, 065 (2015), 1503.01656. (9)
- 592 [108] B. Hespel, D. Lopez-Val, and E. Vryonidou, JHEP **09**, 124 (2014), 1407.0281. (9)
- 593 [109] K. Arnold *et al.*, Comput. Phys. Commun. **180**, 1661 (2009), 0811.4559. (9)
- 594 [110] J. Baglio *et al.*, (2014), 1404.3940. (9)
- 595 [111] T. Binoth *et al.*, Comput. Phys. Commun. **181**, 1612 (2010), 1001.1307, [1(2010)]. (9)
- 596 [112] S. Alioli *et al.*, Comput. Phys. Commun. **185**, 560 (2014), 1308.3462. (9)
- 597 [113] M. Bahr *et al.*, Eur. Phys. J. **C58**, 639 (2008), 0803.0883. (9)
- 598 [114] J. Bellm *et al.*, (2015), 1512.01178. (9)
- 599 [115] W. Buchmuller and D. Wyler, Nucl. Phys. **B268**, 621 (1986). (9)
- 600 [116] K. Hagiwara, S. Ishihara, R. Szalapski, and D. Zeppenfeld, Phys. Rev. **D48**, 2182 (1993). (9, 10)
- 601 [117] O. J. P. Eboli, M. C. Gonzalez-Garcia, and J. K. Mizukoshi, Phys. Rev. **D74**, 073005 (2006), hep-ph/0606118. (9,
602 10)
- 603 [118] C. Degrande *et al.*, Monte Carlo tools for studies of non-standard electroweak gauge boson interactions in multi-
604 boson processes: A Snowmass White Paper, in *Community Summer Study 2013: Snowmass on the Mississippi*
605 *(CSS2013) Minneapolis, MN, USA, July 29-August 6, 2013*, 2013, 1309.7890. (9, 11)

- 606 [119] K. Arnold *et al.*, (2011), 1107.4038. (10)
- 607 [120] K. Hagiwara, R. Szalapski, and D. Zeppenfeld, Phys. Lett. **B318**, 155 (1993), hep-ph/9308347. (10)
- 608 [121] L3, P. Achard *et al.*, Phys. Lett. **B589**, 89 (2004), hep-ex/0403037. (10)
- 609 [122] T. Figy and D. Zeppenfeld, Phys. Lett. **B591**, 297 (2004), hep-ph/0403297. (10)
- 610 [123] V. Hankele, G. Klamke, D. Zeppenfeld, and T. Figy, Phys. Rev. **D74**, 095001 (2006), hep-ph/0609075. (10)
- 611 [124] G. Passarino and M. J. G. Veltman, Nucl. Phys. **B160**, 151 (1979). (10)
- 612 [125] V. D. Barger, K.-m. Cheung, T. Han, and R. J. N. Phillips, Phys. Rev. **D42**, 3052 (1990). (11)
- 613 [126] G. J. Gounaris, J. Layssac, and F. M. Renard, Phys. Lett. **B332**, 146 (1994), hep-ph/9311370. (11)
- 614 [127] A. Alboteanu, W. Kilian, and J. Reuter, JHEP **11**, 010 (2008), 0806.4145. (11, 12)
- 615 [128] W. Kilian, T. Ohl, J. Reuter, and M. Sekulla, Phys. Rev. **D91**, 096007 (2015), 1408.6207. (11, 12)
- 616 [129] W. Kilian, T. Ohl, and J. Reuter, Eur. Phys. J. **C71**, 1742 (2011), 0708.4233. (11)
- 617 [130] M. Moretti, T. Ohl, and J. Reuter, (2001), hep-ph/0102195. (11)
- 618 [131] W. Kilian, T. Ohl, J. Reuter, and C. Speckner, JHEP **10**, 022 (2012), 1206.3700. (11)
- 619 [132] W. Kilian, J. Reuter, S. Schmidt, and D. Wiesler, JHEP **04**, 013 (2012), 1112.1039. (11)
- 620 [133] C. Weiss, B. C. Nejad, W. Kilian, and J. Reuter, PoS **EPS-HEP2015**, 466 (2015), 1510.02666. (11)
- 621 [134] B. C. Nejad, W. Kilian, J. Reuter, and C. Weiss, PoS **EPS-HEP2015**, 317 (2015), 1510.02739. (11)
- 622 [135] N. D. Christensen, C. Duhr, B. Fuks, J. Reuter, and C. Speckner, Eur. Phys. J. **C72**, 1990 (2012), 1010.3251. (11)
- 623 [136] W. Kilian, T. Ohl, J. Reuter, and M. Sekulla, (2015), 1511.00022. (12)
- 624 [137] O. J. P. Eboli, M. C. Gonzalez-Garcia, and S. M. Lietti, Phys. Rev. **D69**, 095005 (2004), hep-ph/0310141. (12)
- 625 [138] F. Bach and T. Ohl, Phys. Rev. **D86**, 114026 (2012), 1209.4564. (12)
- 626 [139] F. Bach and T. Ohl, Phys. Rev. **D90**, 074022 (2014), 1407.2546. (12)
- 627 [140] R. S. Gupta, A. Pomarol, and F. Riva, Phys. Rev. **D91**, 035001 (2015), 1405.0181. (12)
- 628 [141] E. Masso, JHEP **10**, 128 (2014), 1406.6376. (12)
- 629 [142] A. Pomarol, Higgs Physics, in *2014 European School of High-Energy Physics (ESHEP 2014) Garderen, The Netherlands, June 18-July 1, 2014*, 2014, 1412.4410. (12)
- 630 [143] P. Z. Skands *et al.*, JHEP **07**, 036 (2004), hep-ph/0311123. (12)
- 631 [144] B. C. Allanach *et al.*, Comput. Phys. Commun. **180**, 8 (2009), 0801.0045. (12)
- 632 [145] G. D'Ambrosio, G. F. Giudice, G. Isidori, and A. Strumia, Nucl. Phys. **B645**, 155 (2002), hep-ph/0207036. (13)
- 633 [146] C. Degrande, B. Fuks, K. Mawatari, K. Mimasu, and V. Sanz, (2016), in preparation. (13)
- 634 [147] E. E. Jenkins, A. V. Manohar, and M. Trott, JHEP **10**, 087 (2013), 1308.2627. (13)
- 635 [148] E. E. Jenkins, A. V. Manohar, and M. Trott, JHEP **01**, 035 (2014), 1310.4838. (13)
- 636 [149] R. Alonso, E. E. Jenkins, A. V. Manohar, and M. Trott, JHEP **04**, 159 (2014), 1312.2014. (13)
- 637 [150] B. Henning, X. Lu, and H. Murayama, (2014), 1412.1837. (13)
- 638